AerospaceEurope Conference2020
BORDEAUX, FRANCE | 25 - 28 FEBRUARY 2020
CEAS Council of European Aerospace Societies
HOSTED BY: 3AF Association Aéronautique et Astronautique de France

OPTIMAL RECHARGING INFRASTRUCTURE SIZING AND OPERATIONS FOR A REGIONAL AIRPORT

Francesco Salucci, Carlo E. D. Riboldi, Lorenzo Trainelli, Alberto Rolando

Department of Aerospace Science and Technology, Politecnico di Milano,
Via G. La Masa 34, 20156 Milano, Italy. Email: francesco.salucci@polimi.it

KEYWORDS: hybrid-electric propulsion, airport infrastructures, optimal sizing, battery swapping station, plug-in chargers.

ABSTRACT:

A methodology for the optimal sizing and operation of future airport recharging infrastructures for large-scale electric aircraft operations was implemented in the Airport Recharging Equipment Sizing (ARES) tool. ARES can determine the optimal charging schedule and estimate the necessary equipment to smartly charge the batteries which will empower future sustainable aviation segments. Battery plug-in chargers or battery swapping stations are considered as possible charging tools. The sizing is driven by the airport departure schedule and by the technological properties of aircraft and airport, namely batteries and chargers. In this paper, ARES was applied to the case of Athens International Airport, to assess the infrastructures required in case the current schedule of regional flights were operated by a fleet of hybrid-electric aircraft.

1. INTRODUCTION

The introduction of Pure-Electric (PE) or Hybrid-Electric (HE) aircraft fleet in the air transportation system, as envisaged in [1], requires the definition and deployment of a suitable ground infrastructure. Existing airports will have to take into account an increased electric power supply demand, needed to quickly recharge airplane batteries during turnaround times. Indeed, the price of electricity would come to represent a significant cost driver for the airport operator.
Electricity price usually changes significantly over a daily or weekly period – possibly reaching up to two and four times the minimum, respectively, over these time frames, as in the Italian case [2]. A smart scheduling of the recharging activities should therefore be pursued to reduce the energy supply cost.
Such smart recharge planning is clearly connected to the available ground recharging facilities [3,4]. Two basic types of chargers were considered [5], Battery Plug-in Chargers (BPC) and Battery Swapping Stations (BSS), possibly simultaneously present.
BPCs are conceptually similar to refilling stations for fuel. Possible weaknesses of BPCs may arise with large airplanes, whose battery capacity is in the order of several MWh (3.5-7.0 MWh for an aircraft the weight of a B737-800, depending on the mission [6]), leading to very long recharging times, totally unacceptable and incompatible with the usual turnaround time of a liner.
BPCs charging power could be increased to reduce charging time, but, in addition to the procurement cost for the hardware, this would have an impact on the peak power absorbed from the source (typically the grid), which is in turn responsible for a non-negligible fraction of the total cost of energy supply, along with the actual energy acquired. As an example, in the Italian energy supply scenario, the cost of maximum allowed peak power is responsible for 20% of the overall electric energy cost for a typical user [2].
BSS is an alternative to BPC, allowing batteries to be recharged after being disembarked from the aircraft. If an appropriate number of spare batteries is available, a smart scheduling of the recharge can be envisaged, in order to make it compatible with air operations on one hand, and to minimize the power bill on the other. Clearly, more batteries represent a higher procurement cost and an increased logistic effort (batteries must be transported to and from the aircraft, as well as stored safely after recharging and before re-embarking them). Moreover, recharging power for a single BSS, similarly to what happens for BPCs, is limited by technological factors, so a higher number of battery recharges will be needed, resulting in higher acquisition cost.
The energy/power supply required, the number of BPCs and BSSs, and the number of batteries constitute the main output of a sizing problem where the schedule of air operations, i.e. the number of operated flights and their time frames, is given as an input. From the viewpoint of a ground operator, the reconfiguration of an airfield for allowing operations with an PE or HE aircraft fleet should imply defining these outputs, in order to grant minimum procurement and operational costs.
This paper will first outline a comprehensive, original method to solve the problem of optimally sizing the ground infrastructure for future electric air transport. Such method was implemented in the Airport Recharging Equipment Sizing (ARES) tool. An application of ARES to the reconfiguration of the Athens International airport (ICAO code: LGAV) will be presented next. This airport was chosen because it had the largest number of regional aircraft movements in 2018, and electrified versions

of current turboprop regional aircraft (such as ATR 72) are being widely researched on, and their entry in service could reasonably be the first real-world application of PE or HE commercial aviation, as compared to larger liners [7].

2. RECHARGING INFRASTRUCTURE SIZING AND OPERATION: ANALYTIC APPROACH

The airport infrastructure sizing introduced in Section 1 can be analytically modelled as an optimization problem. From an operator standpoint, the optimum represents a balance between the need to grant an assigned operativity level, i.e. a flight schedule, and the necessity of minimizing procurement and operative cost.
In mathematical terms, a suitable cost function J can be built up based on cost chapters as follows:

$$J = C_E + C_P + C_{BSS} + C_{BRS} + C_B \quad (1)$$

where the components C_E, C_P, C_{BSS}, C_{BPC} and C_B represent the cost of the electric energy purchased from the grid, the cost of peak power, the procurement cost of the battery swapping stations and of the plug-in chargers and of the batteries, respectively. In seeking for an optimum of the cost function J, some constraints need to be considered in order to model inherent technological limitations, as well as to mathematically formulate the physics of recharging operations. With the purpose of correctly evaluating the constraints, the dynamics of the infrastructure is integrated over an appropriate time frame of length T. The problem is allocated on a discrete time grid, where the length of each time step is τ.
The cost components and constraint equations will be described in the following subsections, highlighting their respective dependencies.

2.1. Cost components

The cost components in Eq. 1 can be expressed as follows. The cost of energy C_E is bound to the energy amount $E^p(t)$ absorbed from the grid over a given period and to the monetary value per energy unit $\lambda(t)$. Due to the very low frequencies in the evolution of both functions of time (compared to a daytime scale), providing definitions in discrete time is more typical to this type of problem. Therefore, it is possible to write

$$C_E = \sum_{t=0}^{T} \lambda_t E_t^p, \quad (2)$$

where the value of E_t^p represents the energy drained between the current time t and the next one. Clearly, the value calculated in Eq. 2 is a function of the time frame T considered for the analysis. That value should be taken consistently with the definitions of the other components of J, as described through the next equations.

The cost of power can be expressed as

$$C_P = (N_{BSS}P_{BSS} + N_{BRS}P_{BRS})c_P\frac{N_D}{30} \quad (3)$$

where $N_{BSS}, P_{BSS}, N_{BPC}$ and P_{BPC} are the number and nominal power of BSS and BPC, respectively. The sum between braces represents nominal peak power, i.e. the power needed in case all BSS and BPC are operating simultaneously. The term c_P represents the cost per unit peak-power per month, and N_D the number of days in the considered analysis. The value of N_D implicitly defines the limit for the sum in Eq. 1.
The component C_{BSS} represents the procurement cost of the BSS, and can be written as

$$C_{BSS} = N_{BSS}c_{BSS}\frac{N_D}{T_{BSS}} \quad (4)$$

where c_{BSS} is the acquisition cost per unit of the BSS, and T_{BSS} the expected lifespan of the device. Therefore, $\frac{N_D}{T_{BSS}}$ represents the relative extension of the analysis, measured in days, over the expected lifespan of the device. The cost of the unit BSS can be defined based on a technological regression, as a function of P_{BSS} [8].
In a similar fashion, the cost model for BPC can be written as

$$C_{BPC} = N_{BPC}c_{BPC}\frac{N_D}{T_{BRS}} \quad (5)$$

Lastly, the cost model for batteries yields

$$C_B = N_B c_B \frac{N_D}{T_B} \quad (6)$$

where c_B is the acquisition cost per unit battery and $\frac{N_D}{T_B}$ the usual scaling factor.

2.2. Constraints

The parameters influencing the components of the cost function must satisfy an array of constraints, which reflect both technological limitations and models of the recharging processes.
The state of charge $SoC_{i,t}$ of the i-th battery at time index t should be between a minimum SoC^{min} and a maximum SoC^{max}, as defined by technological limits. This is expressed by the following equation,

$$SoC^{min} < SoC_{i,t} < SoC^{max}. \quad (8)$$

Battery charging can be carried out through a BSS or BPC. Battery charging (positive) rate $P_{bat_{i,t}}$ cannot exceed a technological limit expressed by a nominal P_{bat}^{max}. This yields

$$\begin{aligned} 0 < P_{bat_{i,t}}^{BSS} < P_{bat}^{BSS,max}\zeta_{i,t}\phi_{i,t} \\ 0 < P_{bat_{i,t}}^{BRS} < P_{bat}^{BRS,max}\xi_{i,t}\psi_{i,t} \\ \phi_{i,t} + \psi_{i,t} \leq 1 \end{aligned} \quad (9)$$

At any time, a battery can be recharged only if it is connected to a BSS or BPC, and this is implemented by the use of the binary variables $\zeta_{i,t}$ and $\xi_{i,t}$ in Eq. 9, which will be equal to 1 if the battery is connected to a BSS or BPC device respectively, and 0 otherwise. Two separate constraining equations are written, in case the battery is connected to either a BSS or a BPC. Two further binary variables $\phi_{i,t}$ and $\psi_{i,t}$ are added to exclude simultaneous recharging of the same battery from a BSS and a BPC – the value of their sum is constrained below or at unity.
A further constraining equation is represented by the energy balance for the *i*-th battery, yielding

$$SoC_{i,t} = \left(P^{BSS}_{bat_{i,t}} + P^{BRS}_{bat_{i,t}}\right)\tau\eta_c + SoC_{i,t-1} \qquad (10)$$

where η_c is the efficiency of the recharging process. The initial value of the state of charge $SoC_{i,0}$ needs to be assigned. The energy amount drained from the grid and corresponding to the recharge power is

$$E^p_t = \tau \sum_i \left(P^{BSS}_{bat_{i,t}} + P^{BRS}_{bat_{i,t}}\right) \qquad (11)$$

where the sum has to be carried out on the number of active charging devices (BSS and BPC).
Additional binary variables and their corresponding constraints are introduced at an implementation level, to grant global consistency when reducing all constraining equations to a linear form.

2.3. Optimization structure and implementation aspects

The optimization of the cost function in Eq. 1 is carried out with respect to desired operational performance. The flight schedule is assigned over the considered time frame, yielding a number of aircraft that need to be airborne at any collocation point. The number of batteries and recharging devices is then steered by the optimizer to yield the minimum cost as defined by Eq. 1.
Retrieving the expression of J from Eq. 1, we can see that it can be now computed as a function of the optimization variables E^p_t, N_{BSS}, N_{BPC}, N_B and N_{AC}. Other quantities appearing in Eqs. 2 to 7, namely λ_t, P_{BSS}, P_{BPC}, c_P, c_{BSS}, T_{BSS}, c_{BPC}, T_{BPC}, c_{BSS}, c_B, T_B can be considered as assigned technological parameters. Further optimization parameters include the binary variables appearing in Eq. 9, and those required to express all constraints through linear equations. The resulting optimization problem is based on a mix of discrete and non-discrete variables and can be tackled by means of dedicated MIP (Mixed-Integer Programming) solvers.
An analysis on suitably simplified case studies has been carried out first, in order to check whether the problem was well posed and validate results, and to assess the performance of a number of commercial MIP solvers. The selected solution algorithm is GUROBI, which implements a MILP (Mixed-Integer Linear Programming) approach fully compatible with the proposed linear formulation of the optimal problem.

3. RECHARGING INFRASTRUCTURE SIZING AND OPERATIONS AT LGAV AIRPORT

The procedure described in Section 2 can be applied for the determination of the infrastructure requirements for managing PE and HE aircraft fleets at Athens International Airport *Eleftherios Venizelos* (LGAV). LGAV has been selected as a test airport for the sizing procedure, since it was the European airport with the largest number of propeller-driven regional aircraft movements in the five years from 2016 to 2018 [9]. Regional aircraft are widely used to connect Greek islands to the mainland, thus Athens airport makes a perfect test case to assess the infrastructural needs of regional aircraft operation. Three regional airliners were considered for the case study:

1. Bombardier Dash 8 Q400 (78 passengers),
2. ATR42 (~48 passengers),
3. ATR72 (~70 passengers).

This is the class of aircraft that may be interested, in a relatively short term, in the introduction of versions designed to include an HE powertrain, and will therefore include a battery pack.
We supposed to replace the current conventional fleet of aircraft with vehicles that include a serial HE powertrain, and this will have an impact on their mission profile. In fact, taxiing-out, taking-off and climbing up to a defined 'hybrid transition altitude' (3,000 ft in the present case) will be performed in a zero-emission PE mode. Subsequently, the Power Generation System (PGS, i.e. a thermal engine burning hydrocarbon fuel) will be turned on, both for providing energy during final climb and cruise phases and for recharging batteries, if needed. Finally, when descending below the hybrid transition altitude, the PGS will be shut off, so final descent, approach, landing and taxi-in will again be performed in PE mode. This strategy allows a drastically reduction of gaseous and noise emissions at airport level [10].
The technical specifications of the electrified airplanes were obtained by means of the Hyperion preliminary sizing tool developed at the Department of Aerospace Science and Technology at Politecnico di Milano [11–13]. For the sake of clarity, the electrified versions designed by using Hyperion were named as the original model adding an "HE-" prefix, yielding HE-DH8, HE-ATR42 and HE-ATR72 respectively.
Tab. 1 shows the estimated battery capacity for each of the aforementioned models. A budgetary price for the batteries (including cells and battery management system) was calculated using 2018 Lithium-ion battery price, i.e. approximately 176 €/kWh [14]. Even if battery data comes from a

fully-fledged aircraft sizing procedure, they should be taken as representative of a reasonable order of magnitude.

Data coming from public flight tracking services was employed for the study [15]. In particular, flights taking off on Friday, December 13, 2019 ("Friday-only case") and the following weekend ("Weekend case") were used to build the flight schedule to be fed to the optimisation algorithm. The bar plots in Fig. 1 and Fig. 2 depict the relevant departures for the Friday-only case and the Weekend case, respectively. The current fleet of DH8, ATR42 and ATR72 is composed of 10, 9 and 7 airplanes, respectively.

Table 1: Aircraft characteristics

Name	Pax	Battery Price [k€]	Battery capacity [kWh]
HE-DH8	78	253.4	1,400
HE-ATR42	48	184.8	1,000
HE-ATR72	70	237.6	1,300

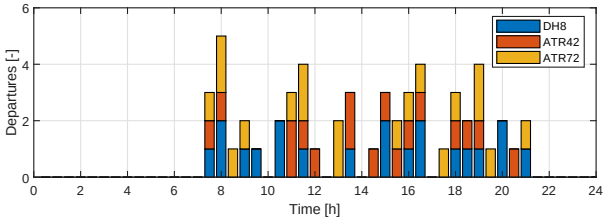

Figure 1: Regional airplane departures from LGAV for the Friday-only case.

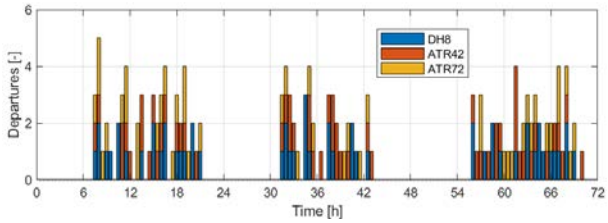

Figure 2: Regional airplane departures from LGAV for the weekend case.

Two different values of the recharge power P_{BSS}, P_{BPC} of the ground recharging devices have been considered: 250 kW and 1,000 kW. These two values were selected as representative of current automotive charging infrastructures. 250 kW is already available for Tesla customers who can use Tesla Superchargers [16], while 1,000 kW are under development to be employed to recharge fully-electric lorries (Tesla MEGACharger [17]).

The cost of the charging devices (c_{BPC}, c_{BSS}) was estimated according to [8]. An additional 10% was added to account for maintenance costs.

Chargers cost, recharge process efficiency η_c, charger life and other data can be found in Tab. 2.

Table 2: Chargers properties

Parameter	Value
c_{BPC}, c_{BSS} 250 kW chargers	66.7 k€
c_{BPC}, c_{BSS} 1000 kW chargers	89.0 k€
Charger life	10 years
Charging efficiency	93 %

Electricity prices in Greece for the year 2018 were assumed for the simulation. They are reported in Tab. 3.

Table 3: Greek electricity prices for the LGAV study case

Energy charge		
0.0648	€/kWh	Daytime
0.0777		Nighttime
Power charge		
10.5080	€/kW/month	Daytime
2.5080		Nighttime

They are composed of a higher Daytime energy charge (from 07:00 to 23:00) and a lower Nighttime energy charge (from 23:00 to 07:00).

3.1. Friday-only case

3.1.1. 250 kW chargers

The resulting consumed electric energy over time, using 250 kW chargers is displayed in Fig. 3.

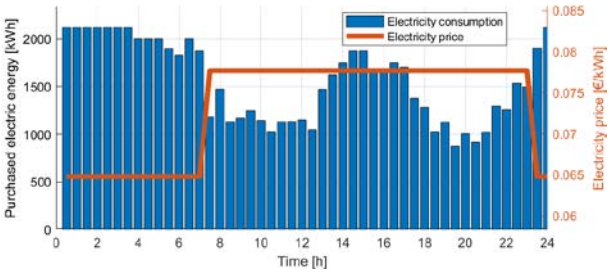

Figure 3: Energy consumption at LGAV, with 250 kW chargers. Friday-only case.

Blue bars represent electric energy absorbed every 30 minutes. The orange line delineates the variation of λ_t during the day. We can see as a greater amount of electricity is drained from the grid during the night, with a quite uniform energy consumption. On the other hand, energy consumption decreases during the day, but still responds to the increases in battery demand.

Fig. 4 portrays the power consumption corresponding to energy usage. The bar plot at the bottom shows the number of batteries recharged at each time step. These batteries can either be charged

with a BSS or with a BPC. In this case, since the aircraft fleet is fixed, an optimally mixed usage of BSS and BPC comes out from ARES.

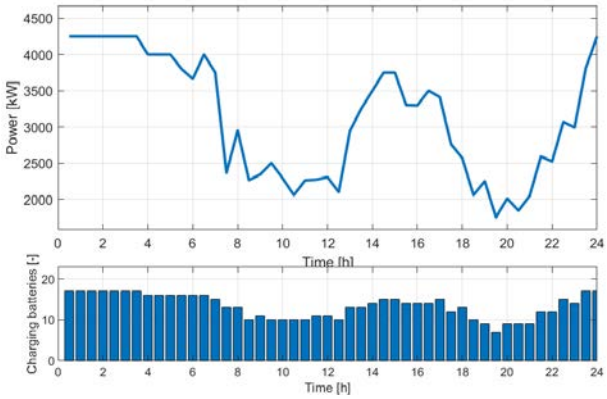

Figure 4: Power consumption (upper graph) and charging batteries (lower graph) at LGAV with 200kW chargers. Friday-only case.

Table 4: LGAV Sizing results. 250 kW chargers. Friday-only case.

Item	Value		
	HE-DH8	HE-ATR42	HE-ATR72
No. airplanes	10	9	7
No. batteries	14	13	13
No. charges	20	17	19
No. BSS	7		
No. BPC	10		
Peak power	4,250 kW		
Energy consumption	74,946 kWh		

Tab. 4 details the outcome of the optimization in terms of resources. It is interesting to note that charging a battery takes between 4.0 and 5.6 hours (depending on the aircraft model) if operating at full power. This recharge time is not compatible with the available aircraft fleet and could impact on the flight schedule. Therefore, BSS charging is employed to recharge some batteries while these are disembarked from the airplane. As a result, seven BSSs are employed together with ten BPCs. The number of batteries is thus 40, to be contrasted with 26 airplanes (14 for the HE-DH8, 13 for the HE-ATR42 and 13 for the HE-ATR72).

3.1.2. 1,000 kW chargers

Fig. 5 depicts the absorbed electric energy in the 1,000 kW charger case. It is immediately clear that the charging process takes place in a shorter amount of time: around 4 times less than the 250 kW case.

No recharges occur between 08:00 and 10:30 avoiding to buy electricity when it is more expensive. On the other hand, Fig. 6 shows that the peak power required in this case is 6 MW. (42% more than in the 250 kW case)

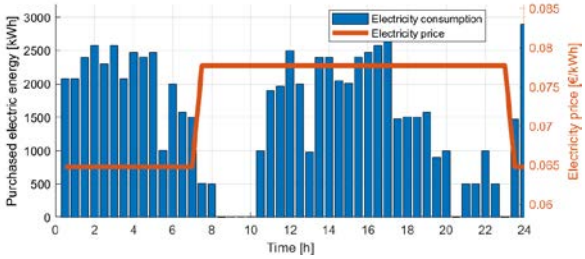

Figure 5: Energy consumption at LGAV, with 1,000 kW chargers. Friday-only case.

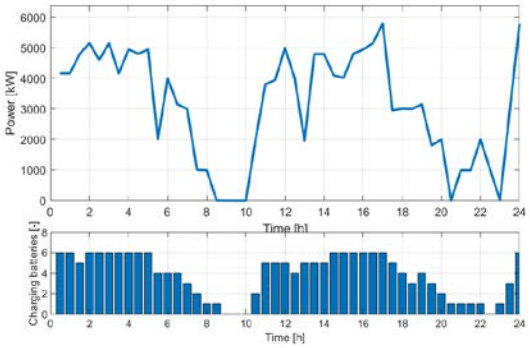

Figure 6: Power consumption (upper graph) and charging batteries (lower graph) at LGAV with 1,000 kW chargers. Friday-only case.

Table 5: LGAV Sizing results. 1,000 kW chargers. Friday-only case.

Item	Value		
	HE-DH8	HE-ATR42	HE-ATR72
No. airplanes	10	9	7
No. batteries	11	9	8
No. BSS	1		
No. BPC	5		
No. charges	20	17	19
Peak power	5,795 kW		
Energy consumption	74,946 kWh		

As a natural consequence of the higher charging power and the reduced charging time, fewer chargers and batteries are needed, as seen from the results detailed in Tab. 5. In particular, only five BPCs and one BSS are used and a minimum of 28 batteries is required to fulfil the battery demand (11 for the HE-DH8, 9 for the HE-ATR42 and 8 for the HE-ATR72), which means that only one extra battery is required for two out of the three airplane models.

3.2. Weekend case

3.2.1. 250 kW chargers

The results for the Weekend case with 250 kW chargers shown in Tab. 6 imply that more batteries are necessary to satisfy the battery demand with respect to the Friday-only case (44 against 40: 15 for the HE-DH8, 15 for the HE-ATR42 and 14 for HE-ATR72). This is probably caused by the large number of airplanes taking off on Sunday night and

the large number of movements in the next morning. Since charging power is limited, and charging time is long, a great number of spare batteries is necessary. In this case a total of 19 chargers are required: 8 BPCs and 11 BSS slots. On the other hand, the large number of chargers and spare batteries allows to lower the peak power (4.75 MW).

Table 6: LGAV Sizing results. 250 kW chargers. Weekend case.

Item	Value		
	HE-DH8	HE-ATR42	HE-ATR72
No. airplanes	10	9	7
No. batteries	15	15	14
No. charges	55	55	44
No. BSS	11		
No. BPC	8		
Peak power	4,750 kW		
Energy consumption	203,441 kWh		

Figs. 7 and 8 depict the energy consumption and power demand during the three days.

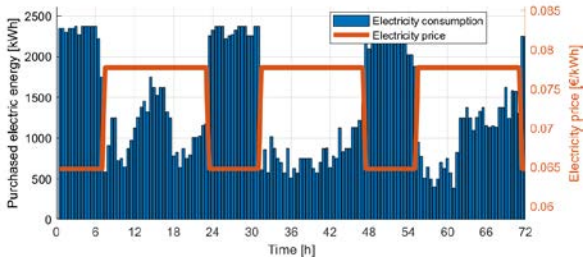

Figure 7: Energy consumption at LGAV, with 250 kW chargers. Weekend case.

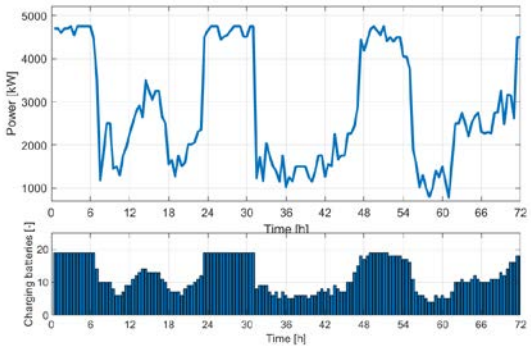

Figure 8: Power consumption (upper graph) and charging batteries (lower graph) at LGAV with 250 kW chargers. Weekend case.

3.2.2. 1,000 kW chargers

Tab. 7 shows the main results obtained when the charging power is raised to 1 MW, in the full weekend case: seven BPCs are employed to satisfy the flight schedule presented in Fig. 2. It is interesting to notice that BSSs are not used. This is a consequence of the fact that charging power is high enough to allow all the 30 batteries to be recharged without being disembarked during the day. However, the minimum number of batteries is higher than the number of flying airplanes. This means that at least three batteries are charged on airplanes that are still on the ground and disembarked afterwards.

Table 7: LGAV Sizing results. 1,000 kW chargers. Weekend case.

Item	Value		
	HE-DH8	HE-ATR42	HE-ATR72
No. airplanes	10	9	7
No. batteries	11	11	8
No. BSS	0		
No. BPC	7		
No. charges	55	55	44
Peak power	6,796 kW		
Energy consumption	203,441 kWh		

Figs. 9 and 10 show how the energy consumption and the demanded power evolve in the full weekend case.

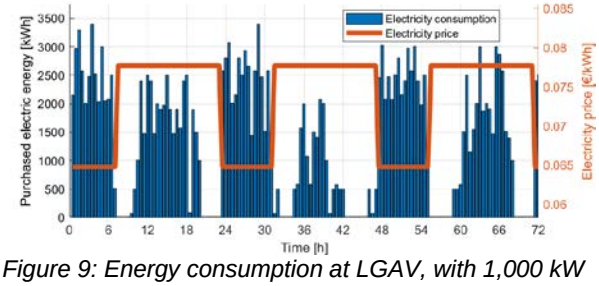

Figure 9: Energy consumption at LGAV, with 1,000 kW chargers. Weekend case.

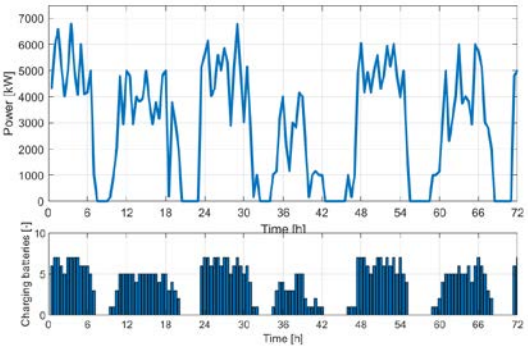

Figure 10: Power consumption (upper graph) and charging batteries (lower graph) at LGAV with 1,000 kW chargers. Weekend case.

By comparing the cost function in the Weekend case, for the two values of charging power, battery cost emerges as the largest part in both the 250 kW and the 1,000 kW case, representing the 61% and 52% of the total respectively. This is shown in Fig. 11, which also shows that the second largest contribution to the cost function is the cost of energy, which is slightly lower in the 1,000 kW case, meaning that it is possible to recharge the batteries in a smarter way, when the electric energy is cheaper. On the other hand, this saving on the

energy leads to an increase in the power cost of electricity, which is less is the 250 kW case. The amount related to chargers is of minor relevance, as it accounts for a very small percentage of the cost function: 4.2 % and 2.6 %, respectively.

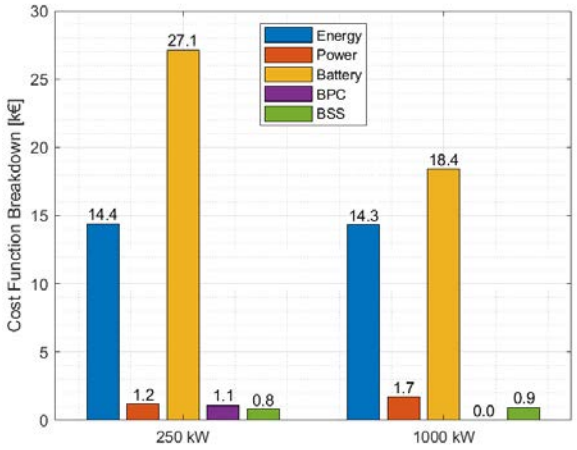

Figure 11: Cost function breakdown for the weekend case

4. CONCLUDING REMARKS

A methodology for the sizing of recharging ground infrastructure in future airports was developed and implemented in the Airport Recharging Equipment Sizing (ARES) tool. ARES minimizes the cost of consumed electric energy as well as acquisition costs for battery recharging devices and batteries, satisfying a pre-determined flight schedule at a given airport. The proposed methodology was applied to Athens International Airport, assuming the replacement of the current regional fleet of ATR 42, ATR72 and DASH 8 with an hypothetical serial HE version of each of these aircraft. The flight schedule employed for the application was taken from actual flight data, publicly available. Two types of chargers were considered: Battery Plug-In Chargers and Battery Swapping Stations. Charging power was set according to current and future values typically found in automotive applications: 250 and 1,000 kW. Results showed that whenever the charging power is limited, i.e. the 250 kW case, recharging times get too long, leading to a large number of required spare batteries. On the other hand, a higher charging power can help in reducing costs but large peak power is required from the grid. Moreover, higher charging power might also impact on the battery life, a factor which has not yet been included in the presented methodology. Future applications of ARES will include this effect, as well as the possibility to add a negative cost bound to putting energy into the grid. The ability to store energy in spare batteries which are not on board, in fact, may grant the ground operator the chance to resell energy to the grid, at times of the day when its value is higher.

5. FUNDING

This research was partially funded by the EU Horizon 2020 research and innovation program, under project MAHEPA, GA N. 723368.

6. REFERENCES

1. Trainelli, L., Bruglieri, M., Salucci, F. & Gabrielli, D. (2020). Optimal Definition of a Short-Haul Air Transportation Network for Door-to-Door Mobility. In Proc. Aerospace Europe Conference (AEC 2020), Bordeaux, France.
2. Servizio Elettrico Nazionale (Italian National Electric Service, visited January 13, 2020). https://www.servizioelettriconazionale.it/
3. Aerospace Standards Committee (2011). Aircraft — Connectors for ground electrical supplies Part 2: Dimensions.
4. Sujitha, S.K. (2016). RES based EV battery charging system: A review. *Renewable and Sustainable Energy Reviews* **75**, 978-988.
5. Zheng, Y., et al. (2014). Electric vehicle battery charging/swap stations in distribution systems: comparison study and optimal planning. *IEEE Transactions on power Systems* **29**, 221–229.
6. Friedrich, C., & Robertson, P.A. (2014). Hybrid-electric propulsion for aircraft. *Journal of Aircraft* **52**, 176–189.
7. de Vries, R., Hoogreef, M., & Vos, R. (2019). Preliminary Sizing of a Hybrid-Electric Passenger Aircraft Featuring Over-the-Wing Distributed-Propulsion. In Proc. AIAA Scitech 2019 Forum, San Diego, CA, USA.
8. Schroeder, A., & Traber, T. (2012). The economics of fast charging infrastructure for electric vehicles. *Energy Policy* **43**, 136–144.
9. Aircraft traffic data by main airport – Eurostat (visited January 13, 2020). https://ec.europa.eu/eurostat/web/transport/data/database
10. Riboldi, C. E. D., Mariani, L., Trainelli, L., Rolando, A. & Salucci, F. (2020). Assessing the Effect of Hybrid-Electric Power-Trains on Chemical and Acoustic Pollution. In Proc. Aerospace Europe Conference (AEC 2020), Bordeaux, France.
11. Trainelli, L., Salucci, F., Rossi, N., Riboldi, C.E.D., & Rolando, A. (2019). Preliminary Sizing and Energy Management of Serial Hybrid-Electric Airplanes. In Proc. AIDAA 2019 XXV International Congress, Roma, Italy.
12. Trainelli, L., Riboldi, C. E. D., Salucci, F., & Rolando, A. (2020). A General Preliminary

Sizing Procedure for Pure-Electric and Hybrid-Electric Airplanes. In Proc. Aerospace Europe Conference (AEC 2020), Bordeaux, France.

13. Rolando, A., Salucci, F., Trainelli, L., & Riboldi, C. E. D. (2020). On the Design of an Electric-Powered Micro-Feeder Aircraft. In Proc. Aerospace Europe Conference (AEC 2020), Bordeaux, France.
14. A Behind the Scenes Take on Lithium-ion Battery Prices – BloombergNEF (visited January 13, 2020). https://about.bnef.com/blog/behind-scenes-take-lithium-ion-battery-prices/
15. ATH/LGAV Athens Eleftherios Venizelos Greece Departures – Flightradar24 (visited January 13, 2020). https://www.flightradar24.com/data/airports/ath
16. Charge on the road – Tesla (visited January 13, 2020). https://www.tesla.com/supercharger?redirect=no
17. Tesla is in talks with electric truck customers to install 'Megacharger' stations, report says – Electrek (visited January 13, 2020). https://electrek.co/guides/tesla-megacharger/